Clean-Breathing: a Novel Sensor Fusion Algorithm Based on ICA to Remove Motion Artifacts from Breathing Signal

1st Luigi Raiano
Università Campus Bio-Medico di Roma
NeXT Lab
Rome, Italy
l.raiano@unicampus.it

2nd Joshua Di Tocco
Università Campus Bio-Medico di Roma
Unit of Measurements
Rome, Italy
j.ditocco@unicampus.it

3rd Carlo Massaroni
Università Campus Bio-Medico di Roma
Unit of Measurements
Rome, Italy
c.massaroni@unicampus.it

4th Giovanni Di Pino
Università Campus Bio-Medico di Roma
NeXT Lab
Rome, Italy
g.dipino@unicampus.it

5th Emiliano Schena
Università Campus Bio-Medico di Roma
Unit of Measurements
Rome, Italy
e.schena@unicampus.it

6th Domenico Formica
Università Campus Bio-Medico di Roma
NeXT Lab
Rome, Italy
d.formica@unicampus.it

***Abstract*—Although smart-textile solutions based on piezoresistive technology have emerged as a tool to assess unobtrusively breathing activity, their signals are affected by the artifacts related to the subjects' movements during common activities (e.g. walking or running). In order to remove such artifacts, we implemented a novel algorithm combining the information recorded by four piezoresistive textile sensors, which allowed to measure rib cage movements due to the breathing activity, with the data synchronously recorded by an inertial measurement unit. Specifically, by using an Independent Component Analysis (ICA), our algorithm allowed to blindly reduce movement artifacts from the signals recorded by the piezo sensors, leading to highlight the breathing activity. We tested our algorithm in a pilot study, in which we enrolled one healthy subject during a free-running task. In order to assess our approach, we compared the signal spectrum obtained applying our algorithm with the one computed after a standard band-pass filter at 0.05-3 Hz. To this aim, we compared the average amplitude of the Power Spectral Densities (PSDs), computed after both approaches, along three frequency ranges: i) [0-1] Hz, related to the breathing activity; ii) [1-2] Hz, related with the torso rotation, during a running a task; iii) [2-3] Hz, related with the pace, during a running a task. Although the study was performed on one single subject, the results obtained seem to be promising. Indeed, within the range [0-1] Hz, the average reduction of the Power Spectral Density (PSD) is only about 4%, while it is considerably higher within frequency range related to the walking/running activity. Specifically, considering the ranges [1-2] Hz and [2-3] Hz such a reduction is around 39% and 36% respectively.**

***Index Terms*—Respiratory Frequency Assessment, Smart Textile, Independent Component Analysis, Sensor Fusion Algorithms.**

This work was partially funded by SENSE-RISC project (ID10/2018) funded by National Institute for Insurance against Accidents at Work (INAIL) and by MONREAB project funded by Fondazione Baroni and H2020/ICT European project CONBOTS ("CONnected through roBOTS: physically coupling humans to boost handwriting and music learning", Grant Agreement no. 871803, call topic ICT-09-2019-2020).

I. Introduction

Wearable systems have gained increasing attention for the continuous monitoring of breathing activities [1], [2]. Specifically, due to their intrinsic characteristic of comfortability and wearability, smart-textile systems based on piezoresistive sensing elements have been successfully used to measure chest wall movements induced by breathing activity, allowing to infer information about respiratory frequency in both healthcare and sport-science applications [3], [4], [5], [6], [7].

Unfortunately, attempting to continuously record the breathing activity, researchers has faced with the problem of the artifacts induced by movements, especially torso rotation and pace [8], [9], leading to the need of developing either devices with negligible sensitivity, with respect such artifacts, or algorithms to remove their contribution in the recorded signals [10]. Concerning the latter solution, to the best of our knowledge, such a problem has been faced employing filtering techniques [8], [11], [12], which filter all those harmonics that piezoresistive (piezo) sensors share with Inertial Measurements Units (IMUs), synchronously recorded. Nonetheless, if the frequency range related to the breathing activity is close to the one related to the movement, the filters implemented will remove also useful signal, hindering to correctly assess the respiratory frequency [8].

The aim of this work is to present a novel algorithm, hereafter called Clean-Breathing (CB), based on Independent Component Analysis (ICA) employed to blindly remove movement artifacts from signals recoded by piezo textile sensors, placed on the thorax of a single subject during a free-running task, combining information recorded synchronously by an IMU [13], [14].

II. Clean-Breathing Algorithm

Independent Component Analysis (ICA) is a technique used to solve the blind source separation problem [15]. In our context, breathing activity can be considered statistically independent from other sources of physiological activity, such as movement artifacts and measurement noise [16]. Moreover, it is known that IMUs are extremely sensitive to body movements induced by physical activity, such as running or walking [17], [18]. Therefore, if the textile and IMU signals were merged and analyzed together, the ICA would theoretically allow to separate the breathing activity (mostly recorded by piezoresistive sensors) from the ones related to the walking/running activity (strongly influencing IMU data).

Let $\boldsymbol{x}$ the vector containing the observations recorded by the smart textile garment and the IMU, the independent components ($\boldsymbol{s}$) can be expressed as:

$$\boldsymbol{s} = \boldsymbol{W}\boldsymbol{x}, \tag{1}$$

with $\boldsymbol{W}$ denoting the mixing matrix, whose coefficients map the contribution of each source to the signal observed. The ICA algorithm is in charge to estimate the vector $\boldsymbol{s}$. Among the independent components (ICs) estimated using (1), the ones which are supposed to arise from physical activity, *i.e.* walking or running, can be discarded when applying the inverse formula to re-compute the vector of the observation as follows:

$$\tilde{\boldsymbol{x}} = \boldsymbol{A}\tilde{\boldsymbol{s}}, \tag{2}$$

with $\boldsymbol{A}$ denoting the inverse or pseudo-inverse of the mixing matrix $\boldsymbol{W}$. Whereas, the symbol $\sim$ over the variables presented in (2) denotes that:

- the vector $\tilde{\boldsymbol{s}}$ has a lower dimension than $\boldsymbol{s}$, since sources of noise may have been removed;
- the vector $\tilde{\boldsymbol{x}}$ has the same dimension of the original vector $\boldsymbol{x}$, but re-computed without possible sources of error.

The main steps of the proposed algorithm, whose flowchart is reported in Fig. 1, can be summarized as follows:

1) To merge IMU and Smart Textile data into a single variable, denoted as $\boldsymbol{x}$.
2) To perform centering and whitening operations before applying the ICA algorithm in order to have zero-mean observations with a covariance matrix equal to the identity one.
3) To run the ICA, implemented through the *FastICA* algorithm [15]. Its implementation in MATLAB™ is available at [19].
4) To evaluate the power spectral densities (*PSDs*) both of the vector $\boldsymbol{s}$ and the IMU data.
5) To select the frequency corresponding to the peaks of the PSD signals related to ICs estimated, hereafter named IC peak frequencies. Specifically, for each IC, we selected all those peaks with an amplitude higher than the 30% of the maximum peak. We selected such a threshold according to prior studies which demonstrated that the contribution of movement-related artifacts can affect up to the 30% of the PSD amplitude [9].
6) To select the peak frequencies of the IMU signals, hereafter named IMU peak frequencies. Specifically, we computed the PSDs both for the accelerometer module (three signals) and the gyroscope one (three signals), and the IMU peak frequencies corresponded to the two highest peaks: one related to the gyroscope, thus mostly related to the thorax rotation; the other one related to the accelerometer, thus mostly related to the pace.
7) To compare the IC peak frequencies with respect the IMU peak frequencies. If an IC peak frequency falls within a range of one of the two IMU peak frequencies ($\pm 0.2Hz$), such an IC is considered strongly affected by movement artifacts and therefore discarded.
8) To re-compute the signal according to Eq. 2, without the discharged ICs.

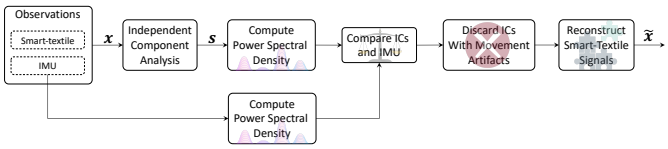

Fig. 1. Flowchart of the algorithm proposed to remove the movement related artifacts from breathing signals measured using piezo textile sensors.

III. Pilot Study

A. Population

We tested the CB algorithm on one single healthy volunteer, without known respiratory problems. The principles of the Declaration of Helsinki and its following amendments were followed in all steps of the study and written informed consent for study participation were obtained. The subject was a male 27-year old, 175 cm height and he had a body mass equal to 77 Kg.

B. Experimental Setup

The system used to collect data consists of a custom printed circuit board with four piezoresistive sensors fixed on two elastic bands, placed on the upper and lower thorax of the subject. According to Fig. 2, each piezo sensor is connected to a dedicated Wheatstone bridge (WB) whose differential output is pre-processed by an Instrumental Amplifier (AD8426 by Analog Devices Inc.) and then digitalized using a 12-bit analog to digital converter (ADC, MAX1237 by Maxim Integrated Inc.; resolution: $8.056 \cdot 10^{-4}$ $\frac{V}{LSB}$) which sends the signal converted to a microcontroller (MCU, STM32F446 by STMicroelectronics Inc.). The PCB embeds also an Inertial Measurement Unit (IMU, LSM9DS1 by STMicroelectronics Inc.) composed of a 3-axis accelerometer (full scale: $\pm 4g$, resolution: 0.122 $\frac{mg}{LSB}$) and a 3-axis gyroscope (full scale: $\pm 245 \frac{deg}{s}$, resolution: 8.750 $\frac{\frac{mdeg}{s}}{LSB}$), which was employed to catch the movement-related artifacts.

Data were recorded with a sampling rate equal to 100 Hz, and locally stored on a micro SD card communicating with the MCU through the SDIO protocol.

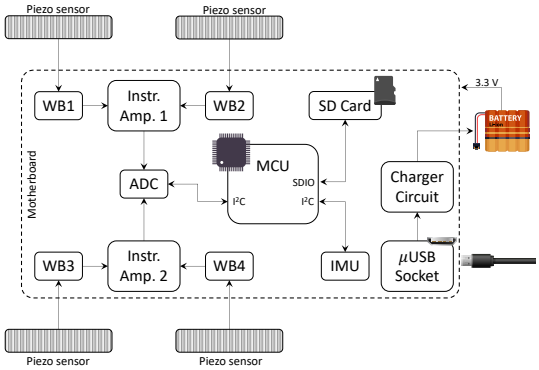

Fig. 2. General Architecture of the electronic system used to carry out the pilot study. A 1-cell Li-Ion battery supplies the board, whose charge is managed by an embedded chip (MCP73831 by Microchip Inc.), connected to the electric network though a micro-USB type-B receptacle.

C. Experimental Protocol

The running task performed by the subject lasted 20 min, of which for data analysis we considered only the last 10 min in order to exclude the adaptation phase to the task. Moreover, the subject was instructed not to move the bands during the task in order to minimize unpredictable artifacts in the recorded signals.

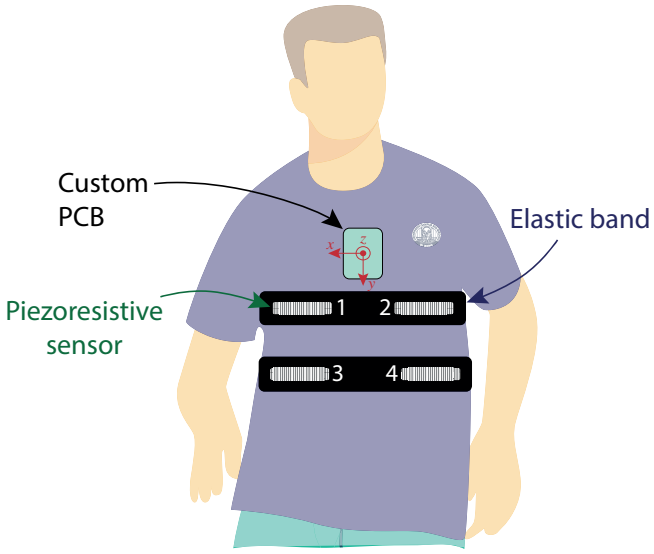

Fig. 3. Garment used to carry out the pilot study. The reference frame represents the one of the IMU.

D. Data Analysis

The Data recorded were post-processed offline in MATLAB™. Firstly, in order to remove the DC offset and high frequency noise we band-pass filtered the data using a 3rd order Butterworth filter between $\{0.05\ Hz,\ 3\ Hz\}$.

Then, we implemented the Clean-Breathing (CB) algorithm presented in section II. In order to quantitatively assess its capability to selectively reduce the movement-related artifacts, we compared the signal processed using the algorithm presented in sec. II, hereafter denoted as *re-computed signals*, with the signals band-pass filtered only, hereafter denoted as *filtered signals*. Specifically, we implemented the following steps:

1) We averaged along the four sensors both the re-computed signals and the filtered ones. We will refer to the average of the re-computed signals along the sensors as *mean re-computed signal*, while as *mean filtered signal* when referring to the average of the filtered ones.
2) We computed the PSD both for resulting signals.
3) We compared the PSD of the *mean filtered signal* and the one of the *mean re-computed signal* both averaged along three frequency ranges:
   - $[0\ Hz,\ 1Hz)$, to which the breathing activity typically belongs [8], [7].
   - $[1\ Hz,\ 2Hz)$, to which the torso rotation during running tasks typically belongs [9].
   - $[2\ Hz,\ 3Hz]$, to which the pace during running tasks typically belongs [20], [21].
4) We computed the percentage reduction factor (ξ) defined as follows:

$$\xi = \frac{P_{filt} - P_{rec}}{P_{filt}} \cdot 100, \tag{3}$$

using the following notation:

- P_{filt}: mean value amplitude of the PSD computed using the *mean filtered signal* along each frequency range.
- P_{rec}: mean value amplitude of the PSD computed using the *mean re-computed signal* along each frequency range.

All PSDs of the signals were computed using the Welch's overlapped segment averaging estimator implemented with the MATLAB's function *pwelch*.

E. Results

The PSDs of the signals recorded by the four piezo sensors are reported in Fig. 4. Firstly, it is evident that the contribution of the channels 1 and 2 resulted to be higher than the one of sensors 3 and 4.

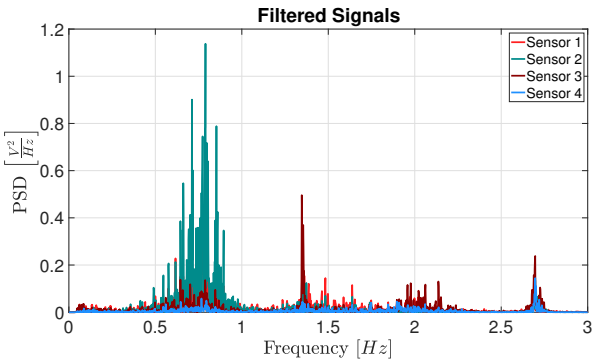

Fig. 4. PSD of the four *filtered signals*.

Moreover, the PSDs presented highlight the contribution of three main groups of frequencies: the first one centered at $\sim 0.7\ Hz$, the second one centered at $\sim 1.3\ Hz$ and the last one, with a significant smaller contribution, centered at $\sim 2.7\ Hz$. Comparing such PSDs with the ones of the accelerometer and the gyroscope (see Fig. 5) and considering the orientation of the IMU reference frame (Fig. 3), the contributions both of the torso rotation (peak at $\sim 1.3\ Hz$ in the y-axis of the gyroscope) and the pace (peak at $\sim 2.7\ Hz$ in the y-axis of the accelerometer) result to be evident, according to [8], [9], [21].

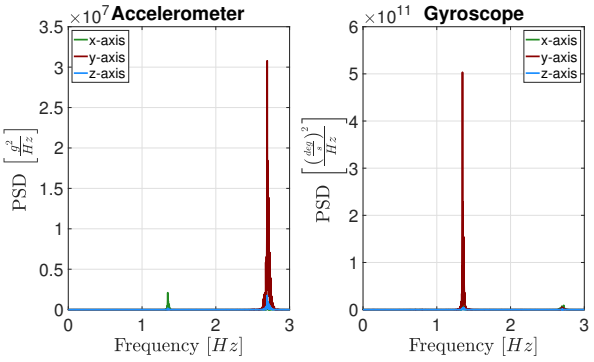

Fig. 5. PSD for each axis of the IMU sensor embedded in the system.

On the other hand, the use of the CB algorithm allowed us to re-compute the piezo signals recorded by selectively reducing the effects of the aforementioned motion artifacts. Indeed, according to Fig. 6, the PSD of the *mean re-computed signal* shows a quite unchanged amplitude within the range $[0\ Hz,\ 1Hz)$ with respect the one of the *mean filtered signal*. Conversely, the amplitude of the *mean re-computed signal* PSD is lower than the *mean filtered signal* one elsewhere.

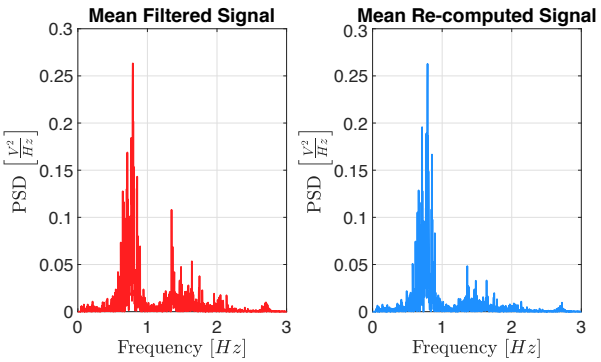

Fig. 6. PSD of the *mean filtered signal* compared with the one of the *mean re-computed signal*.

Such an intuitive aspect is congruent with the quantitative analysis reported in Tab. I. Indeed, the average reduction in the range $[0\ Hz,\ 1Hz)$ is equal to $\sim 4\%$, while it is definitely higher in the other two ranges: $\sim 39\%$ and ~ 36. Interestingly, the amount of noise removed is higher in the range of frequencies related to movement artifacts detected by the IMU, *i.e.* $[1,\ 2)$ and $[2,\ 3]$.

TABLE I
AVERAGE AMPLITUDE BOTH OF THE *mean filtered signal* PSD AND THE *mean re-computed signal*, THE LATTER ONE PROCESSED WITH THE CB ALGORITHM.

Range $[Hz]$	**Filtered PSD** $\left[\frac{V^2}{Hz}\right]$	**re-computed PSD** $\left[\frac{V^2}{Hz}\right]$	**Reduction** $[\%]$
$[0,\ 1)$	$1.7 \cdot 10^{-2}$	$1.6 \cdot 10^{-2}$	~ 4
$[1,\ 2)$	$6.6 \cdot 10^{-3}$	$3.9 \cdot 10^{-3}$	~ 39
$[2,\ 3]$	$1.3 \cdot 10^{-3}$	$8.6 \cdot 10^{-4}$	~ 36

IV. Discussions and Conclusions

We proposed a novel sensor fusion algorithm based on ICA technique to remove the effect of movements in breathing signals recorded by four piezo textile sensors placed on the upper and lower thorax.

We tested the proposed algorithm in a pilot study carried out on one healthy subject during a free-running task. The data were recorded using a wearable system embedding four piezo sensors, fixed on the thorax (see Fig. 3) to capture the breathing activity, connected to a custom PCB which also embeds an IMU to sense running-related parameters, mainly due to thorax rotation and pace.

On the basis of the filtered signal PSDs (see Fig. 4) it is noteworthy that the sensors do not contribute equally to the estimation of the breathing parameters. Indeed, the most reliable sensors are the ones placed on the upper thorax, while the ones on the lower thorax seem to be more noisy. It is unclear whether this effect is due to a bad position of the sensors and it may be interesting to study this paramater, testing different positions of the piezo elements, *e.g.* placing a line of sensors on the thorax and another one on the abdomen.

Although the algorithm was tested only on one single participant, its performance seem to be promising. Indeed, according to Table I the algorithm is capable to finely select in an automatic way the sources of noice, leading to a re-computed signal (eq. 2) characterized by a lower power only within those frequency ranges unrelated with breathing, but strongly affected by torso rotation and pace [22], [7], *i.e.* $[1,\ 2)$ and $[2,\ 3]$. Conversely, within the range $[0,\ 1]\ [Hz]$ the mean value of the PSD remains quite the same.

These results need to be confirmed by collecting more data and comparing them with a respiratory reference signal in order to evaluate in a robust way the actual performance of the CB algorithm. Nonetheless, we may expect that our approach is valuable. Indeed, differently to other algorithms, it does not take into account any classical filtering technique to remove motion artifacts [12], [5], but it removes selectively only the possible sources of motion artifacts, by employing the

ICA technique, which has been widely exploited for similar purposes in different fields [15].

Future works will be devoted to further investigate the performance of the algorithm proposed, carrying out experiments in a structured environment. Specifically, the subjects enrolled will be asked to perform walking/running tasks on a treadmill at different speeds, while recording a respiratory signal reference [9]. Moreover, we will also test whether changing the position of the sensors on the subject can affect the quality of the recorded signals, leading to an improvement of the algorithm itself.

APPENDIX
INDEPENDENT COMPONENTS COMPUTED

The FastICA [19] implemented at step 2 within the CB algorithm (see section II) estimated seven Independent Components (ICs), whose normalized PSDs (nPSDs, each PSD is normalized on the basis of the maximal peak of that specific PSD) are presented in Fig. 7. By comparing the PSDs of each IC, the PSDs of the IMU and the ones of each piezo signal (*filtered signals*), it is possible to make the following considerations:

- Six out of seven ICs (from IC 1 to IC 6) have a strong contribution (higher then 30%, according to point 2 of the CB algorithm) of harmonics with a frequency higher than 1 Hz; therefore such components can be considered as the sources of the artifacts related to running activity.
- Only the seventh IC has a dominant contribution of harmonics with frequencies below 1 Hz and therefore it seems to be the only source of the breathing signal.

Finally, the CB algorithm computed the *re-computed signals* using only the seventh component, on the basis of the conditions described in section II.

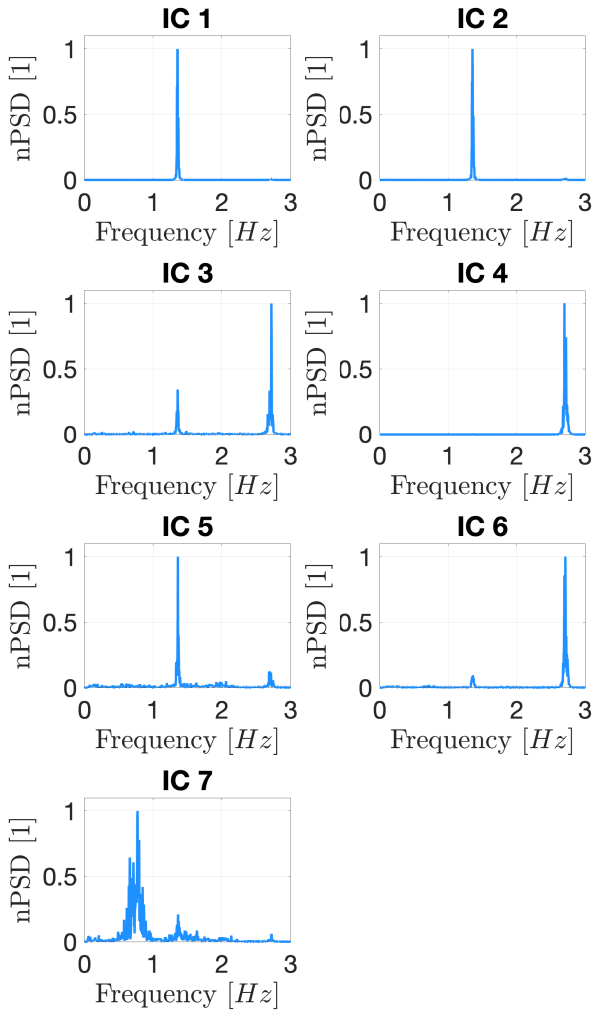

Fig. 7. Normalized PSD (nPSD) of the Independent Components (ICs) computed whithin the CB algorithm.

REFERENCES

[1] T. D. da Costa, M. d. F. F. Vara, C. S. Cristino, T. Z. Zanella, G. N. N. Neto, and P. Nohama, "Breathing monitoring and pattern recognition with wearable sensors," in *Wearable Devices-the Big Wave of Innovation*. IntechOpen, 2019.

[2] G. Aroganam, N. Manivannan, and D. Harrison, "Review on wearable technology sensors used in consumer sport applications," *Sensors*, vol. 19, no. 9, p. 1983, 2019.

[3] C.-T. Huang, C.-L. Shen, C.-F. Tang, and S.-H. Chang, "A wearable yarn-based piezo-resistive sensor," *Sensors and Actuators A: Physical*, vol. 141, no. 2, pp. 396–403, 2008.

[4] J. Jeong, Y. Jang, I. Lee, S. Shin, and S. Kim, "Wearable respiratory rate monitoring using piezo-resistive fabric sensor," in *World Congress on Medical Physics and Biomedical Engineering, September 7-12, 2009, Munich, Germany*. Springer, 2009, pp. 282–284.

[5] A. Nicolò, C. Massaroni, and L. Passfield, "Respiratory frequency during exercise: the neglected physiological measure," *Frontiers in physiology*, vol. 8, p. 922, 2017.

[6] C. Massaroni, J. Di Tocco, D. L. Presti, U. G. Longo, S. Miccinilli, S. Sterzi, D. Formica, P. Saccomandi, and E. Schena, "Smart textile based on piezoresistive sensing elements for respiratory monitoring," *IEEE Sensors Journal*, vol. 19, no. 17, pp. 7718–7725, 2019.

[7] C. Massaroni, J. Di Tocco, M. Bravi, A. Carnevale, D. L. Presti, R. Sabbadini, S. Miccinilli, S. Sterzi, D. Formica, and E. Schena, "Respiratory monitoring during physical activities with a multi-sensor smart garment and related algorithms," *IEEE Sensors Journal*, 2019.

[8] A. Lanatà, E. P. Scilingo, E. Nardini, G. Loriga, R. Paradiso, and D. De-Rossi, "Comparative evaluation of susceptibility to motion artifact in different wearable systems for monitoring respiratory rate," *IEEE Transactions on Information Technology in Biomedicine*, vol. 14, no. 2, pp. 378–386, 2009.

[9] C. Massaroni, J. Di Tocco, D. L. Presti, E. Schena, F. Bressi, M. Bravi, S. Miccinilli, S. Sterzi, U. G. Longo, A. Berton *et al.*, "Influence of motion artifacts on a smart garment for monitoring respiratory rate," in *2019 IEEE International Symposium on Medical Measurements and Applications (MeMeA)*. IEEE, 2019, pp. 1–6.

[10] C. Massaroni, A. Nicolò, D. Lo Presti, M. Sacchetti, S. Silvestri, and E. Schena, "Contact-based methods for measuring respiratory rate," *Sensors*, vol. 19, no. 4, p. 908, 2019.

[11] A. Cesareo, Y. Previtali, E. Biffi, and A. Aliverti, "Assessment of breathing parameters using an inertial measurement unit (imu)-based system," *Sensors*, vol. 19, no. 1, p. 88, 2019.

[12] A. Fedotov, S. Akulov, and A. Akulova, "Motion artifacts reduction in wearable respiratory monitoring device," in *EMBEC & NBC 2017*. Springer, 2017, pp. 1121–1124.

[13] D. Campolo, F. Taffoni, D. Formica, G. Schiavone, F. Keller, and

E. Guglielmelli, "Inertial-magnetic sensors for assessing spatial cognition in infants," *IEEE transactions on biomedical engineering*, vol. 58, no. 5, pp. 1499–1503, 2011.

[14] D. Campolo, F. Taffoni, D. Formica, J. Iverson, L. Sparaci, F. Keller, and E. Guglielmelli, "Embedding inertial-magnetic sensors in everyday objects: Assessing spatial cognition in children," *Journal of integrative neuroscience*, vol. 11, no. 01, pp. 103–116, 2012.

[15] A. Hyvärinen and E. Oja, "Independent component analysis: algorithms and applications," *Neural networks*, vol. 13, no. 4-5, pp. 411–430, 2000.

[16] A. Siqueira, A. F. Spirandeli, R. Moraes, and V. Zarzoso, "Respiratory waveform estimation from multiple accelerometers: An optimal sensor number and placement analysis," *IEEE journal of biomedical and health informatics*, vol. 23, no. 4, pp. 1507–1515, 2018.

[17] H. L. Bartlett and M. Goldfarb, "A phase variable approach for imu-based locomotion activity recognition," *IEEE Transactions on Biomedical Engineering*, vol. 65, no. 6, pp. 1330–1338, 2017.

[18] B. K. Higginson, "Methods of running gait analysis," *Current sports medicine reports*, vol. 8, no. 3, pp. 136–141, 2009.

[19] J. S. Hugo Gävert, Jarmo Hurri and A. Hyvärinen. The fastica package. [Online]. Available: https://research.ics.aalto.fi/ica/fastica/

[20] A. Bhattacharya, E. McCutcheon, E. Shvartz, and J. Greenleaf, "Body acceleration distribution and o2 uptake in humans during running and jumping," *Journal of Applied Physiology*, vol. 49, no. 5, pp. 881–887, 1980.

[21] C. V. Bouten, K. T. Koekkoek, M. Verduin, R. Kodde, and J. D. Janssen, "A triaxial accelerometer and portable data processing unit for the assessment of daily physical activity," *IEEE transactions on biomedical engineering*, vol. 44, no. 3, pp. 136–147, 1997.

[22] D. M. Bramble and D. R. Carrier, "Running and breathing in mammals," *Science*, vol. 219, no. 4582, pp. 251–256, 1983.